Malaysian Journal of Chemistry, 2023, Vol. 25(1), 64-75

The Photocatalytic Activity of Zeolite/TiO_2 Composite for Esterification Reaction of Kapok Seed (*Ceiba pentandra*) Oil

Arief Rahmatulloh* and Mutia Devi Hidayati
Department of Chemical Engineering, Politeknik Negeri Malang, Indonesia
*Corresponding author (e-mail: arief1289@polinema.ac.id)

In this paper, we report on the preparation of a composite based on natural zeolite and titanium dioxide (TiO_2). This composite can act as a bifunctional catalyst for the esterification reaction of kapok seed (*Ceiba pentandra*) oil. TiO_2, which exists as a combination of 90% anatase and 10% rutile, played the role of photocatalyst, while zeolite was the catalyst. The zeolite/TiO_2 composite was obtained by the hydrothermal method. A preliminary analysis of its structure carried out using XRD showed that the addition of TiO_2 did not change the structures of TiO_2 or zeolite. SEM/EDX characterization was performed to determine the distribution of Ti on the surface of the zeolite. The EDX and SEM results confirmed that TiO_2 was successfully loaded onto the surface of natural zeolite. The methylene blue method was used with UV-Vis spectrophotometry to determine the surface area of the composite. A value of 20.866 $m^2 g^{-1}$ was obtained, which indicated that the composite was a good catalyst. The band gap energy of the composite catalyst was 3.0132 eV, which confirmed the presence of TiO_2. The photocatalyst allowed the esterification reaction of kapok seed oil to proceed at 35 °C under UV irradiation. This reaction led to biodiesel conversion. The chemical characteristics of the biodiesel produced were confirmed by GC-MS. Biodiesel properties such as kinematic viscosity, density, flash point and smoke point were determined. The results of the analyses showed that the biodiesel produced met all the specifications of the ASTM D6751 and ASTM D445 biodiesel standards. As a result, the composite zeolite/TiO_2 has good potential as a catalyst for biodiesel conversion.

Keywords: Natural zeolite; titanium dioxide; bifunctional catalyst; esterification; biodiesel

Received: August 2022; Accepted: November 2022

Biodiesel is an alternate fuel produced from renewable raw materials. It consists of various fatty acid esters which can be produced from vegetable oils such as palm oil, coconut oil, castor oil, kapok oil (*Ceiba pentandra*) among others [1,2]. Kapok seed oil is one of the main raw materials that have great potential in biodiesel production. The fact that it is not an edible oil means its availability is more secure, and it is generally disposed of as waste in the cotton industry. Some research on kapok seed oil alcoholysis has been carried out. However, it is still used as a liquid-based catalyst which has weaknesses in terms of the separation and purification process [3]. The ideal catalyst for biodiesel production should have high temperature stability, many strong acid sites, large pores, a hydrophobic surface, as well as be low cost [4]. Hence, heterogeneous solid acid catalysts are preferred in the production of biodiesel to overcome the weaknesses of liquid-based catalysts, such as soap formation and corrosion in the separation process. One of the ways to obtain a heterogenous catalyst is to combine two materials with different properties. A potential heterogeneous catalyst is zeolite [5].

Zeolite is an abundant source of heterogeneous acid catalysts in Indonesia. It can be used in biodiesel production to increase the activity, selectivity and catalytic stability of natural zeolite materials. Baroi *et al.* [6] stated that a zeolite catalyst for the esterification reaction had a free fatty acid conversion rate of 97.2% at 120 °C. To increase its effectiveness and selectivity, zeolite can be combined with other catalysts that can work at low temperatures with good conversion rates. Photocatalytic materials have good potential to be combined with zeolite.

Photocatalysis is a chemical reaction process that uses light as an energy source and takes place at room temperature. One material widely employed in photocatalysis due to its comparatively high photocatalytic activity, low toxicity, chemical stability and low cost, is titanium dioxide (TiO_2). TiO_2 can achieve greater than 95% photocatalytic activity. The utilization of TiO_2 gives several advantages such as an increase in surface area which is directly proportional to catalyst activity [7]. The incorporation of heterogeneous catalysts and photocatalysts in ZnO/SiO_2 composite systems has been investigated by Corro *et al.*[8]. They reported that the photocatalytic activity of the ZnO/SiO_2 composite in the esterification reaction produced a conversion rate of 96%, while the esterification reaction without a photocatalyst only resulted in ~ 3% conversion.

Natural zeolite/TiO_2 (anatase 90:10 rutile) was used as the catalyst in this study because it was more effective than either zeolite or TiO_2 alone. The composite was also able to convert free fatty acids into high methyl esters at a lower cost. As a result, the esterification reactions of kapok seeds could occur optimally [9], [10].

The composite was characterized using XRD (X-Ray diffractometry). Methylene Blue adsorption, confirmed by UV-Vis spectrophotometry, was carried out to determine the surface area of the composite catalyst. The band gap energy of the composite catalyst was analysed using UV-Vis spectrophotometry as well. The photocatalytic activity of the TiO_2/natural zeolite composite material in kapok seed oil was tested in a simple reactor with UV irradiation at 366 nm for 3 hours at 35 °C. The heterogeneous catalyst with TiO_2 was used to investigate its photocatalytic activity toward biodiesel, as well as to determine the best alternative photocatalyst for the manufacture of biodiesel from kapok seed oil.

EXPERIMENTAL

1. Chemicals, Materials and Equipment

1.1. Chemicals and Materials

The composite catalysts used in this study were synthesized from local natural zeolite and titanium dioxide (TiO_2) - anatase (99.99 % purity, Sigma Aldrich, Singapore), while kapok seed oil was obtained from the local cotton industry. Other chemicals used in this study were NaOH (98 % purity, Merck, Singapore), ethanol (99 % purity degree, Merck, Singapore), concentrated NH_4NO_3 (98 % purity, Merck, Singapore), concentrated Na_2SO_4 (97 % purity, Merck, Singapore), methanol (99 % purity, Merck, Singapore), methylene blue (99 % purity, Merck, Singapore), CH_3COOH (97 % purity, Merck, Indonesia), phenolpthalein (PP) indicator, distilled water and Aqua Bidest (double distilled water).

1.2. Equipment

The equipment used in this study included the following: separatory funnel, electric heater, magnetic stirrer, burette, 300 mesh sieve, oven, vacuum desiccator, glass beaker, photoesterification test reactor circuit, furnace (Nabertherm, L 3/12, Germany), density/specific gravity meter (DA-100, Kyoto Electronics), X-ray diffractometer (PanAnalytical Expert Pro), spectrophotometer (Thermo Spectronic 20D+), UV-Vis spectrophotometer (Varian Cary 50), gas chromatograph-mass spectrometer (GC-MS) (Shimadzu QP-2010), scanning electron microscope/energy dispersive X-ray spectrometer (SEM/EDX) (Hitachi S-3000).

2. Preparation and Activation of Natural Zeolite

A sample of natural zeolite was ground to a fine powder and passed through a 300 mesh sieve. Then, 250 g of the natural zeolite powder was soaked in 500 mL Aqua Bidest and stirred for 24 hours. This mixture was filtered and dried in an oven at 100 °C for 24 hours.

Next, 50 g of the dried natural zeolite was mixed with 100 mL of 2 M NH_4NO_3 solution. The mixture was stirred for 4 hours, filtered and then washed with distilled water until the pH of the filtrate turned neutral. The solid obtained was heated at 110 °C for 12 hours and calcined at 400 °C for 4 hours [11].

3. Fabrication of TiO_2-rutile

TiO_2 - anatase powder was manually milled with a mortar for 4 hours. Then, pellets were made from the powder using a ten ton press, and heated in a furnace at a temperature of 1000 °C for 9 hours. The product was analysed by XRD [12].

4. Synthesis of Natural Zeolite/TiO_2 Composite

Activated natural zeolite was quickly stirred into a suspension of TiO_2 sol, a solid phase dispersed in a liquid dispersion medium that does not change its properties easily. A comparison of zeolite photocatalysts has been done by Corro *et al* [8]. The total amount of catalyst required was 2.5 g, which comprised 2.25 g zeolite (90 %) and 0.25 g TiO_2 (10 %). The ratio of anatase : rutile was 0.225 g (90 %) : 0.025 g (10 %). Hence, the ratio of zeolite : anatase : rutile was 2.25 : 0.225 : 0.025 respectively. The mixture was stirred for 2 hours and then placed in a hydrothermal bottle. It was heated at 90 °C in an oven for 16 hours, left to cool at room temperature and filtered. The mixture was then heated for 2 hours in the oven at 100 °C. Finally, the composite samples were activated by calcination at 500 °C for 4 hours in a furnace. The composite catalyst was analysed by both XRD and SEM/EDX. Further characterization utilizing a UV-Vis spectrophotometer was also performed to determine the energy band gap of the composite catalyst.

5. Determination of Surface Area by Methylene Blue Adsorption

The methylene blue adsorption method was used to determine specific surface area. The following steps were performed:

5.1. Determination of Methylene Blue Maximum Wavelength

The absorbance of a 5 ppm methylene blue solution was measured in the range of 380 - 800 nm by UV-Vis spectrophotometry. The optimum wavelength was determined by looking at the largest absorbance or the wavelength which was most strongly absorbed by methylene blue.

5.2. Determination of Operational Time/ Stabilization Time

The operational time was determined by taking 20 mL of 5 ppm methylene blue solution and measuring its absorbance at the maximum wavelength for each time variation of 10, 20, 30, 40, 50, 60, 70, 80 and 90 minutes, respectively. The solution was then measured by a Spectronic 20D+ spectrophotometer. The operational time of the methylene blue complex was determined when the absorbance of methylene blue was stable.

5.3. Determination of Methylene Blue Standard Curve

A series of methylene blue standard solutions were made with concentrations of 1, 2, 3, 4, 5, 6, 7 and 8 ppm, respectively. The maximum absorbance of each solution was measured with a UV-Vis spectrophotometer. Next, a calibration curve of the relationship between concentration and adsorption was plotted, with y as the adsorbance and x as the concentration. Limits of detection (LOD) and limits of quantitation (LOQ) were calculated to validate the standard curve.

5.4. Determination of Optimum Adsorption Time

To determine optimum adsorption time, 20 mL of 16 ppm methylene blue solution was mixed with 0.05 g of the zeolite/TiO_2 - anatase 90:10 rutile composite catalyst. The mixture was shaken at a speed of 150 rpm. Next, the mixture was filtered and the maximum absorbance of the filtrate was measured with a Spectronic 20D+ spectrophotometer at the stabilization time of methylene blue. Finally, the optimum time for the stability of the adsorption of the methylene blue complex was determined.

5.5. Determination of Specific Surface Area of the Composite Catalyst

To determine the specific surface area of composite catalyst, a sample of the 0.05 g zeolite/TiO_2 composite was ground to a powder. Then 20 mL of 16 ppm methylene blue solution was added. The mixture was placed in a shaker at 150 rpm until the absorbance of methylene blue was stable. The mixture was then filtered and the maximum absorbance of its filtrate was measured by UV-VIS spectroscopy [13]. The surface area adsorbed by the composite catalyst was calculated using formula (1) :

$$S = \frac{Xm \times N \times A}{M} \quad (1)$$

where:
S/m^2g^{-1} = specific surface area (m^2/g)
Xm = methylene blue adsorbed by 1 g adsorbent
A = surface area of 1 molecule of methylene blue ($197{,}2\times10^{-20}$ m^2)
N = Avogadro's number ($6{,}02 \times 10^{23}$ molecule/mol)
M = molecular mass of methylene blue (320 g/mol)

6. Esterification of Kapok Seed Oil with Composite Catalyst

The activated natural zeolite/TiO_2 composite with a concentration of 50 % was measured and then mixed with methanol in a three-neck round bottom flask. Then, kapok seed oil was added. The molar ratio of oil to methanol in this process was 1 : 15. Next, the mixture was stirred with a magnetic stirrer and heated at 60 °C. It was then irradiated with a UV lamp at a wavelength of 366 nm for 3 hours at 35 °C. The esterified mixture was placed in a separating funnel and washed with hot water at 80 °C. The product was analysed by GC-MS.

7. Fuel Properties of Biodiesel Derived with the Composite Catalyst

7.1. Determination of Free Fatty Acid Value

A 4 g sample of the biodiesel oil was placed in a flask equipped with a reflux cooler. Then, 10 mL of ethanol was added. Next, the mixture was heated for 30 minutes at 80 °C. After that, the cooled solution was titrated with 0.1 N NaOH solution and PP indicator. Finally, the free fatty acid value was calculated with the following formula:

$$\text{Free fatty acid} = \frac{b \times MNaOH \times 40}{W} \quad (2)$$

b = NaOH volume (mL) used in titration
M_{NaOH} = molarity of NaOH
W = sample weight (g)

7.2. Density Determination

5 mL of the biodiesel sample was injected into a density/specific gravity meter (Kyoto Electronics DA-100) and its density was measured at a temperature of 40 °C.

7.3. Kinematic Viscosity Determination

A 5 mL sample of biodiesel oil was placed in an Ostwald viscometer on a water bath at 40 °C and left for 10 minutes. Next, the time which the sample required to pass through a distance between two marks on the viscometer tube was measured. The viscosity value was calculated with the following formula:

$$v = C \times t \quad (3)$$

v = kinematic viscosity (cSt)
C = viscometer tube constant ($mm^2\ s^{-1}$)s^{-1}
t = the time required for the sample to pass through the capillary tube on the viscometer (s)

7.4. Flash Point Determination

Flash point measurements were carried out according to method D93 (ASTM D6751). A Pensky–Martens closed cup device, containing 65 mL of the sample, was used.

7.5. Cloud Point Determination

5 ml of the sample was placed in a clean and dry test tube, which was carefully put into a freezer. Every 15 minutes, the sample was taken from the freezer and its temperature was measured. If the sample begins to form crystals, it has reached the cloud point.

RESULTS AND DISCUSSION

1. Preparation and Activation of Natural Zeolite

The natural zeolite used in this study contained mordenite as a major structural phase. The purpose of this process was to make natural zeolite more effective as a heterogeneous catalyst. First, natural zeolite was ground and sifted to obtain a powder with a large surface area and homogeneous particle size. This was dried at 110 °C for 24 hours. Next, the prepared natural zeolite was chemically activated to reduce its content of alkali metals, alkaline earth-metals, Fe, Cu, Ni, Zn and other compounds, by mixing it with 2 M NH_4NO_3. This treatment caused NH^{4+} ions to replace the alkali metals on the natural zeolite surface. This fact has been confirmed by Galen Suppes *et al*. [14] who modified zeolite with a metal catalyst. They reported that this exchange was gradual and proportional to the number of available cations. The activated natural zeolite must be washed with distilled water until its filtrate pH becomes neutral. During the washing, NO^{3-} was released from the zeolite and only NH^{4+} ions remained. The next step was physical activation. This treatment releases ammonia gas (NH_3) as the bond between the ammonium group and the active site of the zeolite is susceptible to heating. As a result, hydrogen ions (H^+) were the only substances left on the zeolite surface. In addition, there was a reduction in the weight of the zeolite after calcination, indicating that water and organic compounds had evaporated.

2. Synthesis of Activated Natural Zeolite/TiO_2 Composite

2.1. Phase Transformation of TiO_2 - Rutile from TiO_2 – Anatase

TiO_2 – anatase was ground for 4 hours to transform it into TiO_2 – rutile. This treatment resulted in a fine powder. This powder was formed into pellets in order for the particles to be tightly packed and solid. The TiO_2 pellets were heated at 1000 °C for 9 hours. This treatment initiated the process of atomic migration and resulted in the formation of new bonds between particles. This fact was confirmed by Hanaor and Sorrell, who reported that if the material was crushed, the particles would be broken and become smaller in size. Obtaining a specific polymorph, such as rutile, required treatment of the materials and processing conditions that enhance the formation of rutile. They also revealed that the transition temperature varied in the range of 400 – 1200 °C.[12] The result of this process was the formation of TiO_2 – rutile. X-ray diffraction was used to identify TiO_2 – anatase and TiO_2 – rutile.

The results of the XRD analysis are shown in the diffractograms in Figure 1. The specific crystalline peaks of TiO_2 – anatase appeared at 25.5 °, 37 – 39 °, 48 ° and 54 – 55.5 °. New peaks at $2\theta = 36$ °, 40 °, 41 °, 44.5 °, 55 ° and 57 ° corresponded to TiO_2 – rutile. This fact was confirmed by the shift of the highest peak from 25.5 ° to 27 °, which also indicated that TiO_2 – rutile was successfully formed. Based on these results, it is clear that TiO_2 - anatase had been transformed into TiO_2 - rutile. However, there was still a small amount of the anatase phase, as shown by the peak at $2\theta = 25.2939$ °. The shifting of the diffractogram peaks was caused by structural changes and the length of the TiO_2 crystal lattice. Based on Bragg's law, a change in the crystal structure causes a change in the angle of incidence and the refraction angle of 2θ for X-ray diffraction. The structural changes from anatase to rutile were caused by high temperature heat treatment. At a high temperature, two events occur affecting the formation of the rutile phase: defects in oxygen atoms and the formation of particles. In addition, applying thermal energy causes the Ti-O bond to become longer (Z-out distortion) to infinity and eventually break. The broken Ti-O bond causes the loss of several oxygen atoms. This condition is called an oxygen defect. When the temperature reaches 950 – 1000 °C, a new Ti-O bond is fully formed with a longer bond length and no oxygen defects. As a result, the rutile phase is formed. This fact has been substantiated by Choudhury and Choudhury, who synthesized TiO_2 – rutile from TiO_2 – anatase.[15] They revealed that transformation occurred at the grain interface of the anatase particles. High temperature heating causes interfacial boundary loss of the anatase particles. As consequence, the rutile phases can be formed during the heating process.

2.2. Synthesis of the Natural Zeolite/TiO_2 Composite

TiO_2 – anatase, TiO_2 – rutile and zeolite were added to distilled water and stirred to maximize contact between TiO_2 and zeolite. In this stage, the interactions between TiO_2 and zeolite occurred through the diffusion of TiO_2 into the zeolite pores, which happens faster with stirring.[8] Next, the mixed solution was put into a hydrothermal bottle and heated at 90 °C for 16 hours. This heating treatment aimed to increase the kinetic energy of the modified TiO_2 which diffused into the zeolite pores. TiO_2 in the zeolite pores forms a composite system. The mixing process between TiO_2 and zeolite was carried out with TiO_2 in

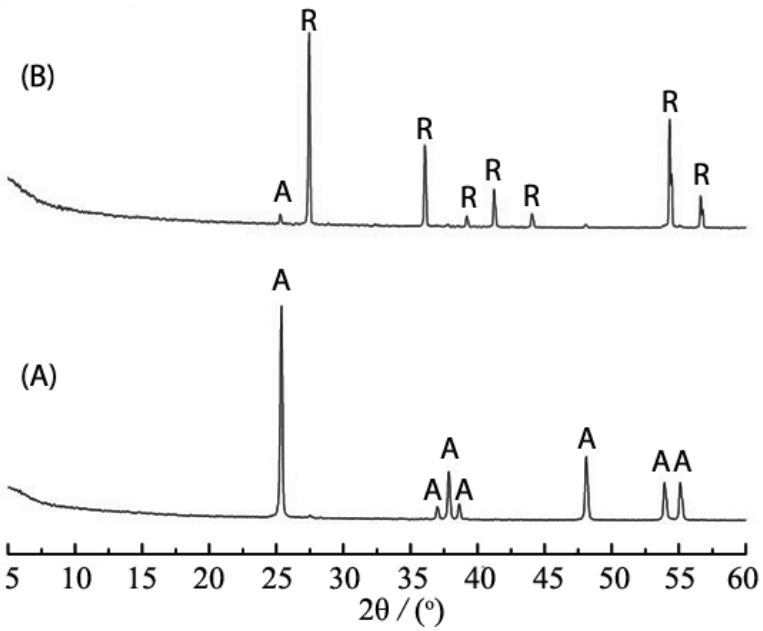

Figure 1. XRD diffractograms of (A) TiO_2 – Anatase and (B) TiO_2 – Rutile

solution form. This condition allows TiO_2 to form a molecular phase, causing it to be pushed into the zeolite pores. As consequence, a solid – liquid reaction occurs which enables the distribution of TiO_2 on the zeolite surface at a moderate temperature (90 °C). This prevents the TiO_2 particles from being distributed deep into the zeolite pores, although they are bonded strongly to the zeolite surface (interface).[10], [16].

Next, the modified product (TiO_2/zeolite) was filtered and heated at a temperature of 100 °C for 2 hours to remove its water content. The sample was then activated at a temperature of 500 °C for 4 hours. This calcination temperature was recommended by Lopez *et al.*[7] Their study revealed that the calcination of TiO_2/zeolite occurred optimally at 500 °C. The zeolite/TiO_2 composite catalyst was analysed using XRD and compared with natural zeolite. The purpose of this characterization was to identify the crystallinity of TiO_2/zeolite and confirm its elemental composition and the distribution of Ti on the zeolite surface. The XRD results can be seen in Figure 2.

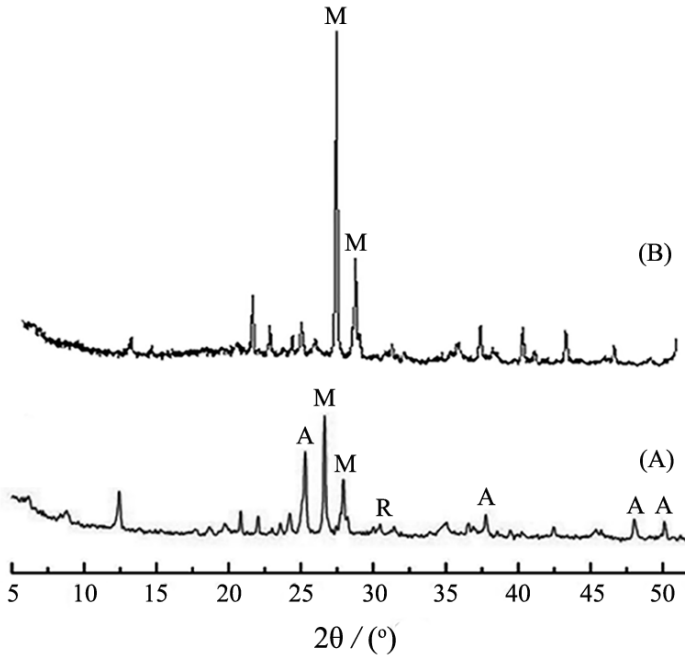

Figure 2. Diffractograms of zeolite/TiO_2-A_{90}:R_{10} (A) and natural zeolite (B) (A = anatase; R = rutile, M = mordenite)

As shown in Figure 2A, the 2θ peaks of TiO_2 – anatase were present at 25.4 °, 37.6 °, 47.9 ° and 50.1 °. However, the characteristic peak of TiO_2 – rutile only appeared at 27.4 °. This was because the mass ratio of TiO_2 – anatase was greater than TiO_2 – rutile. Furthermore, Figure 2B confirms that the mordenite phase was dominant in natural zeolite. This is indicated by the appearance of the characteristic peaks of mordenite at 26.6 ° and 27.9 °, which had the highest intensities. Furthermore, the characteristic peaks of TiO_2 – anatase and rutile (Figure. 2A) indicate that TiO_2 was successfully deposited onto the surface of the zeolite. This is corroborated by the decrease in the intensity of the mordenite peaks in Figure 2A. In addition, the decrease signifies the interaction between natural zeolite and TiO_2. These results are supported by Tedesco *et al.*[17] who loaded TiO_2 onto natural zeolite. They revealed that the differences in the diffractograms of uncoated zeolite and TiO_2-coated zeolite indicated that TiO_2 was successfully loaded onto the surface of natural zeolite.

The immobilization of the anatase and rutile phases of TiO_2 on zeolite did not change the crystal structure of the zeolite or titanium dioxide itself. The diffractogram peaks of TiO_2 – anatase, TiO_2 – rutile and mordenite in natural zeolite indicated that the zeolite and TiO_2 formed a composite system in which both zeolite and TiO_2 retained their individual characteristics. Therefore, it can be used as a bifunctional catalyst in which natural zeolite functions as an acid heterogeneous catalyst and TiO_2 as a photocatalyst. This was affirmed by Lopez *et al.* [7] who synthesized a natural zeolite/TiO_2 composite for photocatalytic degradation. Their study revealed that the structural framework of zeolite remained intact after TiO_2 loading. However, the peaks of zeolite became less intense when in contact with TiO_2. This may be due to the structure of TiO_2 having a greater intensity than zeolite. In addition, the mechanical grinding process preserved the structure of zeolite, as indicated in the XRD diffractograms. The change in peak intensities were due to the milling process when incorporating the materials.

The composite catalyst was then analysed by SEM/EDX to confirm the interaction between natural zeolite and TiO_2. The SEM results can be seen in Figure 3, while the EDX results are shown in Figure 4.

Figure 3 illustrates that natural zeolite (3A) had a smooth and homogeneous surface, as it had no additional material loaded onto it. On the other hand, in Figure 3B, the surface of the zeolite/TiO2 composite catalyst appears rough and textured. This indicates the presence of TiO2 on the composite. The sizes of the TiO2 particles were irregular due to the mix of TiO2 – anatase and TiO2 – rutile on the zeolite surface.[7], [18] This was also confirmed by the EDX analysis (Figure 4). It illustrates the presence of Si, Al, and O atoms, the main components of natural zeolite (A1). The intensity of these atoms were decreased due to their interactions with TiO2 (Figure 4B1). The Ti content was very low and consistent with the content of the composite catalyst. The EDX, SEM and XRD results confirmed that TiO2 was successfully deposited onto the surface of natural zeolite. These results were supported by Tedesco et al.[17] who synthesized a zeolite/TiO2 composite as a biogas enhancer. They found that deposition of the titanium dioxide coating did not exhibit a significant effect on the substrate morphology and was typically uniformly distributed. Furthermore, their EDX result also indicated that TiO2 was successfully added to zeolite.

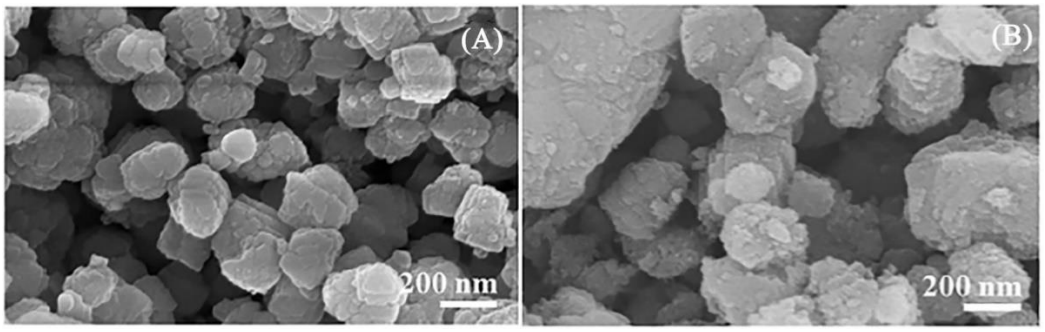

Figure 3. SEM micrographs of natural zeolite (A) and the zeolite/TiO_2 composite catalyst (B)

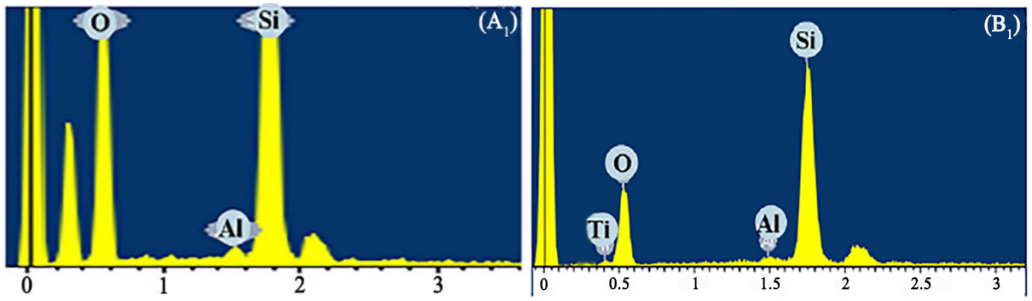

Figure 4. EDX results for natural zeolite (A_1) and the zeolite/TiO_2 composite catalyst (B_1)

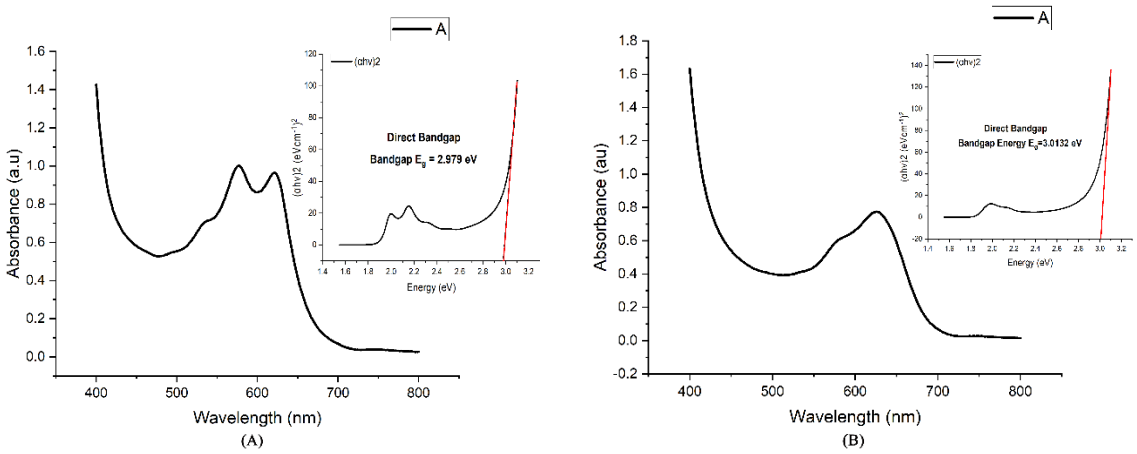

Figure 5. Band gap energy calculations for TiO_2 (A) and the zeolite/TiO_2 composite catalyst (B)

3. Calculation of the Zeolite/TiO_2 Composite Catalyst Energy Band Gap

The calculation of the energy band gap for the composite catalyst utilized UV-Vis spectroscopy spectra, and the Tauc Plot method. The aim of band gap energy calculation is to confirm the effect of photocalytic TiO_2 addition on the structure of the zeolite/TiO_2 composite catalyst. The results of this calculation can be seen in Figure 5:

Figure 5 shows that the band gap energy of TiO_2 was 2.979 eV, while that of the composite catalyst was 3.0132 eV. These results indicate that the presence of TiO_2 increased the band gap energy of zeolite due to the incorporation of TiO_2 into the zeolite structure. Further, the increase in the band gap energy of the zeolite/TiO_2 composite catalyst was related to the widening of the valence and conduction bands. The increase also corresponded with the TiO_2 loaded on the zeolite [19]. This fact was corroborated by Lopez *et al.* [7] who synthesized TiO_2 and a Mexican natural zeolite composite (T/MZ). They found that loading TiO_2 into zeolite increased the band gap energy of the composite.

4. Surface Area Analysis using the Methylene Blue Adsorption Method

Methylene blue is a cationic dye with strong adsorption powers. Therefore, implementing this method is a good way to determine the adsorption capacity of TiO_2/ zeolite. As a result, the surface area of the TiO_2/zeolite sample can be measured as well.[15], [20].

4.1. Determination of Methylene Blue Maximum Absorption Wavelength

When the absorbance is at its maximum, the sensitivity becomes maximum as well, and the change in absorbance for each unit of concentration is the largest.[21] In our experiments, the maximum absorption of methylene blue occurred at a wavelength of 664.0 nm (Figure 5).

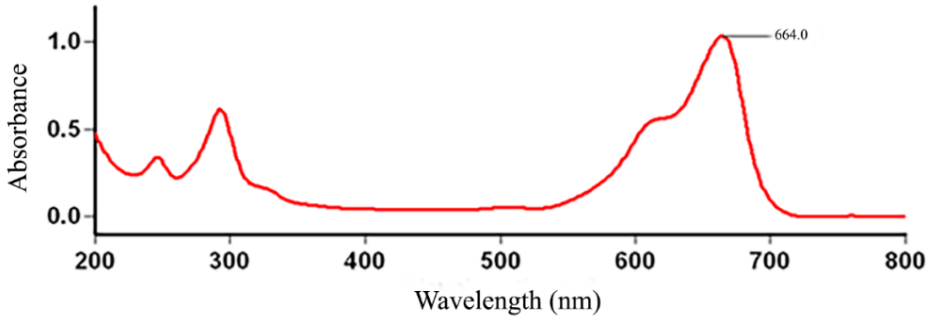

Figure 5. Maximum absorption of methylene blue

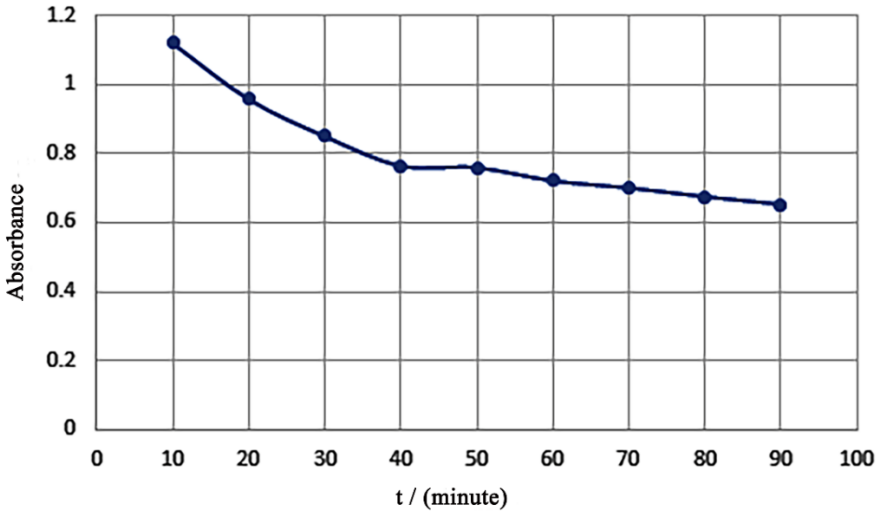

Figure 6. Operational time of methylene blue

4.2. Determination of Operational Time/ Stabilization Time

Determination of operational time defines the most stable measurement time. It is determined by measuring the relationship between measurement time and the absorbance of the solution. Figure 6 shows that methylene blue was stable at 40 - 50 minutes. Therefore, the surface area of the composite material was determined within that time period.

4.3. Obtaining a Methylene Blue Standard Curve

A standard curve was obtained by making standard solutions with concentrations of 1 to 8 ppm. The absorbance of each solution was measured. Using this data, a curve was plotted to show the relationship between absorbance (y) and concentration (x). The slope or gradient of the curve is considered to be the molar absorptivity. Based on Figure 7, it can be seen that there was a directly proportional relationship between absorbance and concentration. The higher the concentration, the higher the absorbance.

Based on the regression equation, the LOD value of this method was 0.496829095 ppm. This is the lowest value of methylene blue which can be detected with this method and distinguished from the mean of the blanks. The LOQ of this method was 1.656096983 ppm. This value was the lowest concentration of analyte which could be defined with good recovery and accuracy using this method.

4.4. The Determination of Optimum Adsorption Time

0.05 g of TiO_2/zeolite composite material was placed in an Erlenmeyer shaker coated with aluminium foil, to which 20 mL of 16 ppm methylene blue was added. The concentration of methylene blue should be high enough to produce a driving force to push methylene blue molecules into the TiO_2/zeolite composite material. The shaker was coated with aluminium foil to protect the methylene blue from being degraded by light.

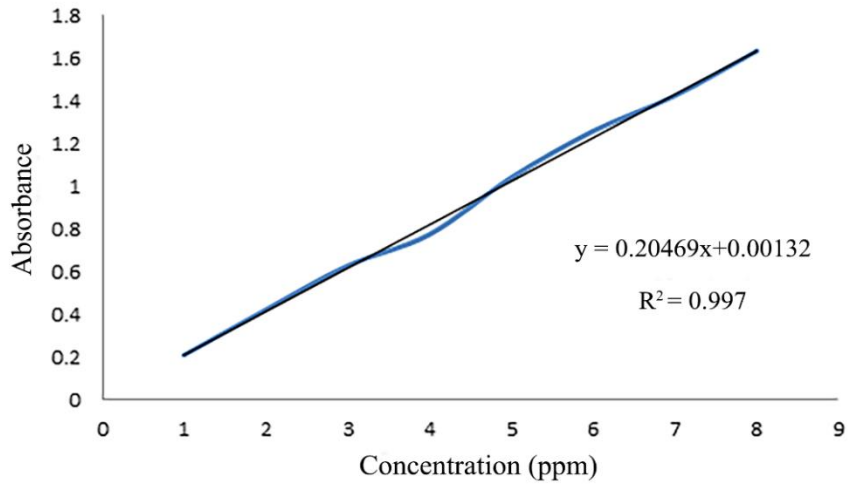

Figure 7. Standard Curve of Methylene Blue

The mixture was shaken for 40 to 50 min at 150 rpm. The time variation was carried out around the stabilization time of the methylene blue complex. The time variation aimed to determine the amount of TiO_2/zeolite composite material that had maximally adsorbed methylene blue to a saturation point. The optimum adsorption was found to occur at 40 min with 20.8660 $m^2 g^{-1}$ of methylene blue surface area, when methylene blue reacted with the surface of the composite material. Thus, it was assumed that the pores and the outer surface of the catalyst were completely filled with methylene blue molecules. The amount of methylene blue adsorbed was proportional to the surface area of the composite catalyst material. The surface area of methylene blue at 50 min decreased to 18.7818 $m^2 g^{-1}$. All surface areas of methylene blue were calculated using formula (1). Khanday *et al.* reported that the decrease in the surface area of the composite material was due to desorption of methylene blue molecules from the active surface of the composite material [20].

4.5. Determination of Specific Surface Area of the Composite Catalyst

The determination of the specific surface area of the TiO_2/zeolite composite material was carried out by varying the optimum adsorption time. According to Rianto *et al*.,[22] the surface area of the TiO_2/zeolite composite material was measured by using an area approach of each methylene blue molecule of 197.2 × 10^{-20} m^2. Each mole of methylene blue consists of 6.02 × 10^{23} molecules (Avogadro's number). As a result, the surface area of the TiO_2/zeolite composite catalyst can be found using this approach. The specific surface area of the TiO_2/zeolite composite catalyst calculated using formula (1) was 20.8660 $m^2 g^{-1}$. This indicates that the TiO_2 material applied to the zeolite was evenly distributed. As a result, the material had a good surface area to be used as a catalyst.

5. Esterification of Kapok Seed Oil with the Composite Catalyst

The natural zeolite/TiO_2 composite functions as a catalyst in the esterification reaction of biodiesel synthesis from kapok seed oil. The catalyst is used to convert free fatty acids in kapok seed oil into alkyl esters. By doing so, it reduces the free fatty acid content. The treatment reduces soap formation occurring during the esterification reaction. Before the process, kapok seed oil was prepared through a heating and filtering process. The heating treatment minimized the water content in the kapok seed oil, which was then filtered through filter paper. Therefore, the oil was free from solid impurities.

The activity of the TiO_2/zeolite composite catalyst was tested by mixing kapok seed oil with methanol (acting as a reactant) at a molar ratio of 1:12. Methanol was used in excess to obtain a better conversion at room temperature. Next, the catalyst was added into the mixture, which was then stirred with a magnetic stirrer and irradiated with a UV lamp at a wavelength of 365 nm for 3 hours at 35 °C to accelerate the reaction. UV irradiation was used to activate TiO_2 anatase:rutile as a photocatalyst [18]. This allowed the reaction to proceed at 35 °C. With UV irradiation, the reaction was conducted successfully in 3 hours. When irradiation was continued, the reaction temperature increased, and the reaction turned into a saponification reaction [23]. The reaction of free fatty acids (ALB) with methanol is as follows:

$$RCOOH_{(aq)} + CH_3OH_{(aq)} \rightarrow RCOOCH_{3(aq)} + H_2O_{(aq)}$$

The biodiesel product was then analysed by GC-MS to identify its chemical characteristics. The GC-MS spectrum obtained is displayed in Figure 8.

Figure 8 shows the range of compounds present in the biodiesel sample. Identification of the compounds was carried out by estimating the fragmentation patterns of each peak using mass spectral data. One of the compounds had a retention time (Rt) between 35.7–36.7 minutes with a base peak similar to the methyl ricinoleic $(C_4H_8)^+$ standard at *m/z* 55, the largest component in kapok seed oil. The characteristic methyl ricinoleate fragmentation was confirmed by the presence of high-intensity peaks at *m/z* 55 and 166. McLafferty's rearrangement was shown by the peak at *m/z* 74 $(C_3H_6O_2)^+$. This was confirmed by Naureen *et al*.,[24] who analysed biodiesel obtained from sun-flower oil. Their study revealed that the base peak in all saturated free fatty acids was observed at *m/z* 74 which was a product of the well-known McLafferty rearrangement process. Other components had very similar fragmentation patterns with characteristic peaks at *m/z* 55 (base peak), [M-32]+ due to loss of methanol (the methoxy group plus hydrogen atom) and [M-74]+ due to the loss of the McLafferty ion.

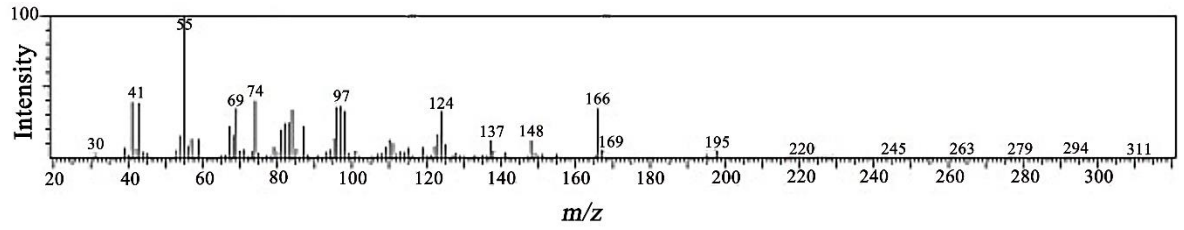

Figure 8. Total ion chromatogram of kapok seed oil biodiesel

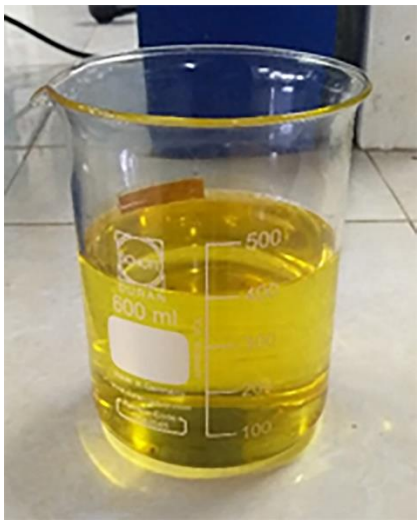

Figure 9. Biodiesel product of kapok seed oil

6. Fuel Properties of Biodiesel Derived with the Zeolite/TiO_2 Composite Catalyst

6.1. Free Fatty Acids

The biodiesel oil (methyl ester) produced was pale yellow and transparent, as shown in Figure 9. During the separation process, methyl ester was the top layer in the separatory funnel, while glycerol was the bottom layer. The methanol remained after the transesterification reaction combined with the methyl ester and glycerol. Subsequently, the free fatty acid content of the biodiesel oil was analysed by titration using 0.1 N NaOH solution with PP indicator. The result obtained was 0.27 % NaOH/g. The ASTM D6751 standard allows a maximum of 0.5 % NaOH/g free fatty acid in biodiesel. This indicates that the biodiesel oil produced in this study fulfilled the requirements of the ASTM D6751 biodiesel quality standard.

6.2. Kinematic Viscosity

Kinematic viscosity is the main parameter in determining the quality of methyl esters because it has a major influence on the effectiveness of methyl esters as a fuel. Vegetable oil has a viscosity far above that of diesel fuel. This prevents the direct use of vegetable oil as a fuel. One of the main objectives of esterification is to reduce the viscosity of vegetable oil so that it can meet diesel fuel standards. The kinematic viscosity of the methyl ester produced in this study was 2.55 cSt. The ASTM D445 biodiesel quality standard specifies that the kinematic viscosity of biodiesel at a temperature of 40 °C should range from 1.9 to 6.0 cSt [25]. Therefore, it can be concluded that the biodiesel oil produced in this study met this quality standard requirement.

6.3. Density

Density can determine if a transesterification reaction is successful. ASTM D6751 states that the density of biodiesel should range from 0.860 to 0.900 g cm^{-3}. A previous study found that the methyl ester of kapok seed oil with a 99.6 % ester content had a density of 0.879 at 15 °C[8]. The density of the biodiesel produced in this study was 0.890 g cm^{-3}, thus fulfilling the requirements of the ASTM D6751 biodiesel quality standard.

6.4. Flash Point

The flash point of biodiesel is used as a mechanism to limit the level of unreacted alcohol remaining in the finished fuel. It is normally specified to meet fire regulation requirements. A high flash point facilitates the storage of fuel, because the oil will not burn easily at room temperature. According to ASTM D6751, the flash point of biodiesel should be higher than 130 °C [26]. The flash point of the kapok biodiesel was found to be 187 °C, which meets the quality standard requirement.

6.5. Cloud Point

The cloud point is the point or temperature at which calm smoke or mist occurs at the bottom of a test tube. The maximum cloud point of biodiesel according to the standard is 18 °C or 291 K [27]. The kapok biodiesel oil had a cloud point at a temperature of 11 °C or 284 K. Thus, the kapok biodiesel oil fulfilled this requirement of the ASTM D445 biodiesel quality standard.

Based on these results, the zeolite/TiO_2 (anatase 90:10 rutile) composite can be utilized as a catalyst for the esterification reaction of biodiesel. This is supported by Sabzevar *et al*. who stated that ZIF-8/TiO_2 could be a recoverable and efficient catalyst for esterification. [10] However, further investigation needs to be done on the physical and chemical characteristics of the composite catalyst to ensure its effectiveness.

CONCLUSION

A natural zeolite/TiO_2 composite material was successfully synthesized. The TiO_2 which was applied to the zeolite material was found to be evenly distributed. Characterization by XRD showed that the TiO_2 distribution on the composite material did not change the structures of TiO_2 and zeolite. The SEM and EDX results confirmed that TiO_2 was successfully deposited onto the surface of the natural zeolite. The composite material had a surface area of 20.8660 $m^2 g^{-1}$ which is good surface area to utilize as a catalyst. The band gap energy of the composite catalyst was 3.0132 eV, which confirmed the existence of the photocatalyst on the composite. UV irradiation was used to activate TiO_2 anatase: rutile as a photocatalyst, and this allowed the reaction to proceed at 35 °C. The chemical characteristics of the biodiesel were confirmed by its GC-MS spectra which exhibited high-intensity peaks at *m/z* 166 and 55. The free fatty acid content of the biodiesel was 0.27 % NaOH/g, which fulfilled the ASTM D6751 biodiesel quality standard requirement. The physical characteristics of the biodiesel produced, namely kinematic viscosity, density, flash point and cloud point, all complied with the requirements of the ASTM D6751 and ASTM D445 biodiesel standards as well. As a result, the composite zeolite/TiO_2 has excellent potential to be used as a catalyst for biodiesel conversion.

ACKNOWLEDGEMENTS

The authors would like to express their gratitude to the Chemical Engineering Department of Politeknik Negeri Malang for extending their support and providing the infrastructure to carry out their research work.

REFERENCES

1. Athar, M. and Zaidi, S. (2020) A review of the feedstocks, catalysts, and intensification techniques for sustainable biodiesel production. *J. Environ. Chem. Eng.*, **8(6)**, 104523. doi: 10.1016/j.jece. 2020.104523.

2. Syafiuddin, A., Chong, J. H., Yuniarto, A. and Hadibarata, T. (2020) The current scenario and challenges of biodiesel production in Asian countries: A review. *Bioresour. Technol. Reports*, **12**, July, 100608. doi: 10.1016/j.biteb.2020. 100608.

3. Puna, J. F., Correia, M. J. N., Dias, A. P. S., Gomes, J. and Bordado, J. (2013) Biodiesel production from waste frying oils over lime catalysts. *React. Kinet. Mech. Catal.*, **109(2)**, 405–415. doi: 10.1007 /s11144-013-0557-2.

4. Lotero, E., Liu, Y., Lopez, D. E., Suwannakarn, K., Bruce, D. A. and Goodwin, J. G. (2005) Synthesis of biodiesel via acid catalysis. *Ind. Eng. Chem. Res.*, **44(14)**, 5353–5363. doi: 10.1021/ie049157g.

5. Narasimhan, M., Chandrasekaran, M., Govindasamy, S. and Aravamudhan, A. (2021) Heterogeneous nanocatalysts for sustainable biodiesel production: A review. *J. Environ. Chem. Eng.*, **9(1)**, 104876. doi: 10.1016/j.jece.2020.104876.

6. Baroi, C. and Dalai, A. K. (2014) Esterification of free fatty acids (FFA) of Green Seed Canola (GSC) oil using H-Y zeolite supported 12-Tungstophosphoric acid (TPA). *Appl. Catal. A Gen.*, **485**, 99–107. doi: 10.1016/j.apcata.2014.07.033.

7. Piedra López, J. G., González Pichardo, O. H., Pinedo Escobar, J. A., de Haro del Río, D. A., Inchaurregui Méndez, H. and González Rodríguez, L. M. (2021) Photocatalytic degradation of metoprolol in aqueous medium using a TiO2/ natural zeolite composite. *Fuel*, **284**, March, 119030. doi: 10.1016/j.fuel.2020.119030.

8. Corro, G., Pal, U. and Tellez, N. (2013) Biodiesel production from Jatropha curcas crude oil using ZnO/SiO2 photocatalyst for free fatty acids esterification. *Appl. Catal. B Environ.*, **129**, 39–47, doi: 10.1016/j.apcatb.2012.09.004.

9. Alvarez, K. M., Alvarado, J., Soto, B. S. and Hernandez, M. A. (2018) Synthesis of TiO2 nanoparticles and TiO2-Zeolite composites and study of optical properties and structural characterization. *Optik (Stuttg).*, **169**, May, 137–146. doi: 10.1016/j.ijleo.2018.05.028.

10. Moatamed Sabzevar, A., Ghahramaninezhad, M. and Niknam Shahrak, M. (2021) Enhanced biodiesel production from oleic acid using TiO2-decorated magnetic ZIF-8 nanocomposite catalyst and its utilization for used frying oil conversion to valuable product. *Fuel*, **288**, February, 119586. doi: 10.1016/j.fuel.2020.119586.

11. Trisunaryanti, W., Triwahyuni, E. and Sudiono, S. (2005) Preparasi, Modifikasi Dan Karakterisasi Katalis Ni-Mo/Zeolit Alam Dan Mo-Ni/Zeolit Alam. *Teknoin*, **10(4)**, 269–282. doi: 10.20885/ teknoin.vol10.iss4.art7.

12. Hanaor, D. A. H. and Sorrell, C. C. (2011) Review of the anatase to rutile phase transformation. *J. Mater. Sci.*, **46(4)**, 855–874. doi: 10.1007/s10853-010-5113-0.

13. Kahr G. and Madsen, F. T. (1995) Determination of the cation exchange capacity and the surface area of bentonite, illite and kaolinite by methylene blue adsorption. *Appl. Clay Sci.*, **9(5)**, 327–336. doi: 10.1016/0169-1317(94)00028-O.

14. Suppes, G. J., Dasari, M. A., Doskocil, E. J., Mankidy, P. J. and Goff, M. J. (2004) Transesterification of soybean oil with zeolite and metal catalysts. *Appl. Catal. A Gen.*, **257(2)**, 213–223. doi: 10.1016/j.apcata.2003.07.010.

15. Choudhury, B. and Choudhury, A. (2013) Local

structure modification and phase transformation of TiO2 nanoparticles initiated by oxygen defects, grain size, and annealing temperature. *Int. Nano Lett.*, **3(1)**, 1–9. doi: 10.1186/2228-5326-3-55.

16. Xie, W., Huang, X. and Li, H. (2007) Soybean oil methyl esters preparation using NaX zeolites loaded with KOH as a heterogeneous catalyst. *Bioresour. Technol.*, **98(4)**, 936–939. doi: 10.1016/j.biortech.2006.04.003.

17. Tedesco, S., Hurst, G., Imtiaz, A., Ratova, M., Tosheva, L. and Kelly, P. (2020) TiO2 supported natural zeolites as biogas enhancers through photocatalytic pre-treatment of Miscanthus x giganteous crops. *Energy*, **205**, 117954. doi: 10.1016/j.energy.2020.117954.

18. Nagarjuna, R., Roy, S. and Ganesan, R. (2015) Polymerizable sol-gel precursor mediated synthesis of TiO2 supported zeolite-4A and its photo-degradation of methylene blue. *Microporous Mesoporous Mater.*, **211**, 1–8, doi: 10.1016/j.micromeso.2015.02.044.

19. Rahman, A., Nurjayadi, M., Wartilah, R., Kusrini, E., Prasetyanto, E. A. and Degermenci, V. (2018) Enhanced activity of Tio2/natural zeolite composite for degradation of methyl orange under visible light irradiation. *Int. J. Technol.*, **9(6)**, 1159–1167. doi: 10.14716/ijtech.v9i6.2368.

20. Khanday, W. A., Marrakchi F., Asif, M. and Hameed, B. H. (2017) Mesoporous zeolite–activated carbon composite from oil palm ash as an effective adsorbent for methylene blue. *J. Taiwan Inst. Chem. Eng.*, **70**, 32–41. doi: 10.1016/j.jtice.2016.10.029.

21. Setthaya, N., Chindaprasirt, P., Yin, S. and Pimraksa, K. (2017) TiO2-zeolite photocatalysts made of metakaolin and rice husk ash for removal of methylene blue dye. *Powder Technol.*, **313**, 417–426. doi: 10.1016/j.powtec.2017.01.014.

22. Rianto, L. B., Amalia, S. and Khalifah, S. N. (2013) Pengaruh Impregnasi Logam Titanium Pada Zeolit Alam Malang Terhadap Luas Permukaan Zeolit. *Alchemy*, **2(1)**, 58–67. doi: 10.18860/al.v0i0.2295.

23. Guo, M. *et al.* (2021) Process optimization of biodiesel production from waste cooking oil by esterification of free fatty acids using La3+/ZnO-TiO2 photocatalyst. *Energy Convers. Manag.*, **229**, September, 113745. doi: 10.1016/j.enconman.2020.113745.

24. Naureen, R., Tariq, M., Yusoff, I., Chowdhury, A. J. K. and Ashraf, M. A. (2014) Synthesis, spectroscopic and chromatographic studies of sunflower oil biodiesel using optimized base catalyzed methanolysis. *Saudi J. Biol. Sci.*, **22(3)**, 332–339. doi: 10.1016/j.sjbs.2014.11.017.

25. Sarin, A., Sharma, N., Devgan, K. and Singh, M. (2020) Study of kinematic viscosity and density of biodiesels exposed to radiations. *Mater. Today Proc.*, **46**, 5516–5522. doi: 10.1016/j.matpr.2020.09.257.

26. Aziz, I., Nurbayti, S. and Ulum, B. (2012) Pembuatan produk biodiesel dari Minyak Goreng Bekas dengan Cara Esterifikasi dan Transesterifikasi. *J. Kim. Val.*, **2(3)**, 443–448, doi: 10.15408/jkv.v2i3.115.

27. Mejía, J. D., Salgado, N. and Orrego, C. E. (2013) Effect of blends of Diesel and Palm-Castor biodiesels on viscosity, cloud point and flash point. *Ind. Crops Prod.*, **43(1)**, 791–797. doi: 10.1016/j.indcrop.2012.08.026.